Mechanical properties of interacting lipopolysaccharide membranes from bacteria mutants studied by specular and off-specular neutron scattering

Emanuel Schneck,[1,2] Rafael G. Oliveira,[2,*] Florian Rehfeldt,[2,†] Bruno Demé,[3] Klaus Brandenburg,[4] Ulrich Seydel,[4] and Motomu Tanaka[1,2,‡]

[1]*Biophysical Chemistry II, Institute of Physical Chemistry and BIOQUANT, University of Heidelberg, D69120 Heidelberg, Germany*

[2]*Department of Physics, Technical University Munich, D85748 Garching, Germany*

[3]*Institut Laue-Langevin, 6 Rue Jules Horowitz, F38042 Grenoble Cedex 9, France*

[4]*Research Center Borstel, D23845 Borstel, Germany*

(Received 11 March 2009; revised manuscript received 3 September 2009; published 28 October 2009)

Specular and off-specular neutron scattering are used to study the influence of molecular chemistry (mutation) on the intermembrane interactions and mechanical properties of the outer membrane of Gram-negative bacteria consisting of lipopolysaccharides (LPSs). For this purpose, solid-supported multilayers of mutant LPS membranes are deposited on silicon wafers and hydrated either at defined humidity or in bulk buffers. The planar sample geometry allows to identify out-of-plane and in-plane scattering vector components. The measured two-dimensional reciprocal space maps are simulated with membrane displacement correlation functions determined by two mechanical parameters (vertical compression modulus and bending rigidity) and an effective cutoff radius for the membrane fluctuation wavelength. Experiments at controlled humidity enable one to examine the influence of the disjoining pressure on the saccharide-mediated intermembrane interactions, while experiments in bulk buffers (i.e., in the absence of an external osmotic stress) reveal the effect of divalent cations on LPS membranes, highlighting the role of divalent cations in the survival mechanism of bacteria in the presence of antimicrobial molecules.

DOI: 10.1103/PhysRevE.80.041929 PACS number(s): 87.16.dj, 25.40.Dn, 87.18.Fx, 87.14.Cc

I. INTRODUCTION

Lipopolysaccharides (LPSs) are the main component of the outer leaflet of the outer membrane of Gram-negative bacteria [1] acting as a protection layer against the surrounding. It was found in several *in vivo* studies [2–4] that bacteria are resistant against the intrusion of cationic antimicrobial peptides in the presence of divalent cations (Ca^{2+}, Mg^{2+}). This phenomenon has been drawing increasing attention in the last years since it is of fundamental importance for the understanding of the mode of action of a class of antibacterial drugs [5]. In our recent account [6], we utilized the combination of grazing-incidence x-ray scattering and Monte Carlo simulations to reveal the structural origin of the barrier capability of LPS rough mutants against cationic antimicrobial peptides (herring protamine). Divalent cations condense near the inner core of the LPSs, leading to the collapse of saccharide chains, which prohibits the intrusion of the peptides.

To date, LPSs with various structural complexities have been investigated using x-ray diffraction experiments, including crystallographic studies on the molecular structure [7–9] and small-angle scattering studies on the polymorphisms of the molecules in bulk buffers [10–12]. Small-angle x-ray scattering from isotropic lipid suspensions [13–17] enables the determination of characteristic length scales of membrane multilayers at various temperatures in the presence of different ion species, but the random orientation of membranes generally does not allow for the identification of momentum transfers perpendicular and parallel to the membrane planes. This problem can be overcome by the deposition of lipid multilayers on planar substrates [18–21]. Information on the structure normal to the sample plane can be obtained from specular scattering, whereas the membrane fluctuation characteristics (reflecting the mechanical properties of interacting membranes) can be extracted from off-specular signals. To date, this approach has mainly been used for synthetic lipid membranes [22–25], but also for natural membranes [26] as well as for lipid-peptide and lipid-protein mixtures [27,28] and lipid-cholesterol mixtures [29].

Although Snyder *et al.* [12] deposited multilayers of several LPS types on solid substrates, they merely measured their lamellar periodicities at various conditions. Recently, we demonstrated that specular and off-specular neutron scattering can quantitatively reveal the significant influence of molecular structures (glycosidic junctions) on the intermembrane potential (compression modulus) and the bending rigidity of synthetic glycolipid membranes, which suggested the applicability of this strategy for more complex natural glycolipids [30]. Katsaras and co-workers studied solid-supported LPS multilayers using specular neutron scattering to deduce the vertical structure (perpendicular to the membrane plane) of LPS membranes at relative humidities up to 85% [31,32]. However, there has been no experimental study that utilizes off-specular scattering to determine quantitatively the mechanical properties of LPS membranes.

In the present paper, we carried out a systematic investigation of the influence of molecular complexity on the mechanical properties of interacting LPS membranes using

*Present address: CIQUIBIC-UNC, Ciudad Universitaria X5000HUA Córdoba, Argentina.

†Present address: Georg-August-Universität, III. Physikalisches Institut, 37077 Göttingen, Germany.

‡Corresponding author; tanaka@uni-heidelberg.de

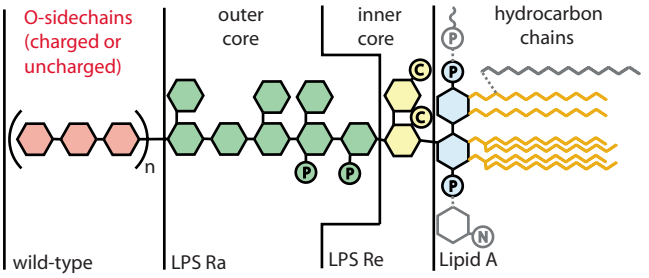

FIG. 1. (Color online) Molecular structures of the studied molecules. Starting from Lipid A, the basic building block, the structures show a systematic increase in complexity. A certain fraction of Lipid A and LPS Re molecules contain an extra palmitoyl chain, a 4-amino-deoxyarabinose, and a phosphatidylethanolamine. P, C, and N denote phosphate, carboxylate, and amino groups, respectively.

specular and off-specular neutron scattering. At first, measurements were performed with a temperature-controlled climate chamber at defined osmotic pressures, ranging from 8×10^6 to 2.5×10^8 Pa (corresponding to 95%–20% relative humidity). Furthermore, the influence of divalent cations on intermembrane interactions and bending rigidities was examined by measurements in bulk buffers.

II. MATERIALS AND METHODS

A. LPS molecules

LPS Ra and LPS Re molecules were purified [33] from the bacterial strains *R*60 and *R*595 of *Salmonella enterica* sv. Minnesota. Lipid A is a hydrolysis product [34] of LPS Re, since LPS Re is the simplest LPS with which bacteria can be cultured [10,35].

The chemical structures of the studied molecules are presented in Fig. 1. They can be considered as basic structures of wild-type lipopolysaccharides. Lipid A is the fundamental building block of more complex LPS molecules. It consists of two negatively charged phosphorylated glucosamines bound to six hydrocarbon chains. LPS Re possesses two more negatively charged 2-keto-3-deoxyoctonoic acid (KDO) units, constituting the "inner core" of all LPSs. In addition to that, LPS Ra possesses eight more saccharide units, two of which are phosphorylated [36]. This moiety is known as "outer core." Compared to wild-type LPSs, the LPS Ra only lacks the O-polysaccharide (O-side chain), which is known to be highly polydisperse [37]. In addition to the invariant part described above, a certain fraction of Lipid A and LPS Re molecules contain further substitutions, such as an extra palmitoyl chain, a 4-amino-deoxyarabinose, and a phosphatidylethanolamine [1]. The previously reported values [10] of molecular weight, number of phosphate or carboxylate groups, and chain melting temperature T_m of each molecule are summarized in Table I.

B. Chemicals, sample preparation

Lipid A and LPS Re were dissolved in 7:3 mixtures (v/v) of chloroform and methanol at a concentration of 2 mg/mL. Since LPS Ra cannot easily be dissolved in organic solvents, it was suspended in pure water at a concentration of 2 mg/mL. A 0.5 mL portion of solution/suspension was deposited onto a rectangular (55×25 mm^2) Si(100) substrate with native oxide (Si-Mat, Landsberg/Lech, Germany), which was cleaned by a modified RCA method [the silicon substrates were cleaned by successive ultrasonication in acetone, ethanol, and methanol and subsequent immersing in a solution of 1:1:5 (v/v/v) H_2O_2(30%)/NH_4OH(30%)/water at 60 °C for 30 min] [38]. During the process of solvent evaporation, the amphiphilic molecules self-assemble into planar membrane stacks, aligned parallel with the substrate surface. To remove residual solvent, the wafers were stored at 70 °C for 3 h and subsequently in a vacuum chamber overnight. The average number of membranes in the stacks was at the order of several hundreds, as can be calculated from the amount of solution and the coated area. To cancel the thermal history of the samples, at least two heating-cooling cycles between 20 °C and 70 °C were repeated at a high relative humidity ($h_{\mathrm{rel}}>95\%$) and the samples were stored at 4 °C overnight prior to the measurements. Since all LPS molecules used in this study are hydrogenated, the samples were hydrated either by D_2O vapor or by buffers containing 100% D_2O (Euriso-Top, Saint-Aubin, France) to achieve the maximum contrast in scattering length density between hydrated saccharide head groups and hydrocarbon chains. The "Ca^{2+}-free buffer" contained 100 mM NaCl and 5 mM Hepes at pH 7.4, while the "Ca^{2+}-loaded buffer" additionally contained 5 mM $CaCl_2$. For some special cases, experiments were carried out in the presence of 50 mM $CaCl_2$. All other chemicals were purchased from Fluka (Taufkirchen, Germany) and used without further purification.

C. Neutron scattering

Neutron scattering experiments were carried out at the D16 diffractometer of the Institut Laue-Langevin (ILL, Grenoble, France). Figure 2 shows the geometry of the

TABLE I. Physical characteristics (molecular weight, number of phosphate or carboxylate groups, and chain melting temperature) of the studied molecules [10].

	Molecular weight	Number of phosphate or carboxylate side groups	Bilayer chain melting temperature
Lipid A	1797g/mol	2	46 °C
LPS Re	2237g/mol	4	30 °C
LPS Ra	3835g/mol	6	36 °C

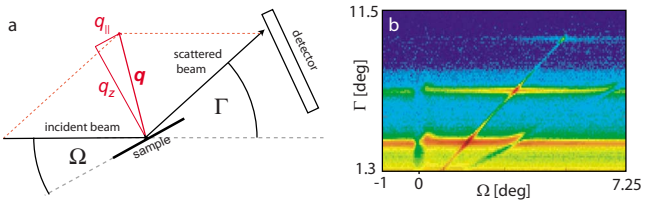

FIG. 2. (Color online) (a) Geometry of the scattering experiments and (b) scattering intensity from LPS Ra multilayers as a function of Γ and Ω, measured at 60 °C and ~95% relative humidity. From geometrical considerations, the angular coordinates Γ and Ω can be translated into the reciprocal space coordinates q_z and $q_\parallel$ [Eq. (1)].

experiment (top view). A monochromatic neutron beam ($\Delta\lambda/\lambda=1\%$) of $\lambda=4.54$ Å or $\lambda=4.73$ Å reaches the sample through the aluminum windows of the sample chamber, while the incident angle Ω (i.e., the angle between the incident beam and the sample plane) is adjusted by a rotation stage. The intensity of the beam diffracted from the sample is recorded by a position-sensitive ^{3}He two-dimensional (2D) detector with 128×128 channels. Γ denotes the angle between the scattered and the incident beams. The sample was rotated stepwise with respect to the incident beam. The beam width was 2 mm horizontally and 25 mm vertically. For each measurement at an angle Ω, the detector readout was normalized to the intensity of the incident beam (via an in-beam monitor), the channel sensitivity, and the illuminated sample area. Subsequently, the 2D detector readout was integrated in the vertical direction, which results in a one-dimensional intensity projection as a function of the horizontal detector channel position (corresponding to Γ). Thus, one Ω scan yielded the recorded intensity as a function of Ω and Γ. This is shown in Fig. 2 for LPS Ra multilayers at 60 °C and ~95% relative humidity. The data sets in angular coordinates can be transformed into reciprocal space maps by geometrical considerations

$$q_z = \frac{2\pi}{\lambda}[\sin(\Gamma-\Omega)+\sin(\Omega)],$$

$$q_\parallel = \frac{2\pi}{\lambda}[\cos(\Gamma-\Omega)-\cos(\Omega)]. \quad (1)$$

Here, q_z and $q_\parallel$ denote the scattering vector components perpendicular and parallel to the sample plane (see Fig. 2 left), i.e., the coordinates of the reciprocal space.

D. Sample environment

For measurements in humidified air, a climate chamber provided by the ILL was used, which allows for the precise regulation of both sample temperature and relative humidity (i.e., the osmotic pressure exerted to the sample) [30]. To ensure the equilibration, the sample was kept at each temperature and humidity condition for at least 30 min before the measurement. For experiments in bulk buffers, a self-built liquid cell was used. A sketch is shown in Fig. 3. The liquid cell consists of two rectangular Si wafers (55

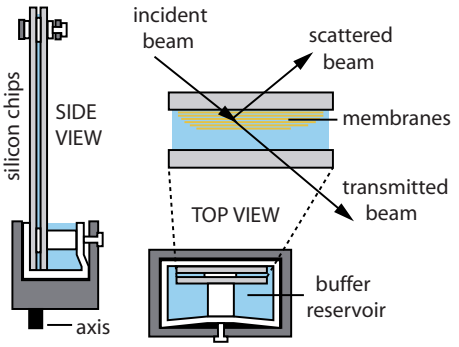

FIG. 3. (Color online) Sketch of the self-developed liquid cell. The solid-supported membrane multilayers are immersed in a thin layer of bulk buffer between the two silicon wafers. The neutron beam reaches the sample through the silicon support.

$\times25$ mm^2), one of which is coated with the membrane stacks. The wafers are separated by glass slide pieces (thickness 0.10 mm) and the capillary force confines a thin layer of aqueous buffer between the two wafers. As shown in the sketch, the neutron beam reaches the membrane multilayers through the silicon support. During measurements, the entire liquid cell was kept inside the climate chamber at controlled temperature and high relative humidity (>95%) to minimize the evaporation of water.

E. Simulation of the scattering signals based on mechanical parameters

In the first step, realistic sets of membrane displacement correlation functions were modeled in a continuum model approximation based on the discrete smectic Hamiltonian [18]. Within this framework, the vertical compressibility of the membrane stacks is characterized by the compression modulus B, while the stiffness of the membranes against bending is characterized by the membrane bending modulus κ. The correlation functions $g_k(r)$ can be expressed with the Caillé parameter η and the de Gennes parameter λ of smectic liquid crystals [18]. Here, $k=0$ corresponds to the membrane self-correlation and $k>0$ to the cross-correlations of the membranes with their kth neighbors. r denotes the in-plane distance between two considered points. As shown in our previous paper [30], the effect of the finite sample size can be taken into account by introducing an effective cutoff radius R, which coincides with an upper limit for the wavelength of the membrane fluctuations. Mathematically, R defines a lower integration limit in the calculation of the correlation functions [Eq. (2)] and enables us to generate realistic correlation functions to describe the studied samples

$$g_k(r) = \frac{d^2}{\pi^2}\eta\int_{2\pi/R}^{\infty}\frac{[1-J_o(q_\parallel r)\exp(-\lambda k q_\parallel^2 d)]}{q_\parallel\sqrt{1+\frac{\lambda^2 d^2}{4}q_\parallel^4}}dq_\parallel,$$

$$\text{where}\quad \eta=\frac{\pi k_B T}{2d^2\sqrt{\kappa B/d}}\quad\text{and}\quad \lambda=\sqrt{\frac{\kappa}{Bd}}. \quad (2)$$

The lamellar periodicity d can be obtained experimentally from the positions of the Bragg peaks and the correlation

functions are fully determined by the three free parameters η, λ, and R.

The scattering signals were modeled in kinematic approximation, which assumes that the intensity of the scattered beam is much weaker than the incident illumination. Therefore, only the second Bragg sheets were considered to guarantee the validity of this assumption. In kinematic approximation, the scattering from periodical membrane stacks which possess correlated roughness can be expressed as a function of the displacement correlation functions $g_k(r)$ [30,39]

$$S(q_z,q_\parallel) \propto \frac{1}{q_z^2}\left[N\int_{-\infty}^{\infty} \exp[-q_z^2 g_0(r)/2]e^{-iq_\parallel r}dr + 2\sum_{k=1}^{N}(N-k)\cos(kq_z d) \times \int_{-\infty}^{\infty} \exp[-q_z^2 g_k(r)/2]e^{-iq_\parallel r}dr \right]. \quad (3)$$

Based on this expression, the scattering signals were modeled in the angular coordinates of the experiment to maintain a uniform grid of points both in experimental and simulated data sets. Instrumental resolution was included by convolution of the signal in Ω and Γ direction with a Gaussian function, representing the point spread function of the measurement resulting from the finite angular width and the wavelength spread of the neutron beam. In the simulations, the parameters η, λ, and R were varied to minimize deviations from the experimental results for (i) the Γ-integrated Bragg sheet intensity and (ii) the Γ width of the sheets simultaneously. Subsequently, the mechanical parameters κ and B were calculated from η and λ.

III. RESULTS AND DISCUSSION

All measurements were conducted at 60 °C, which is more than 10 °C above the chain melting temperature of all studied molecules (see Table I), so that we can ensure all the systems to be in fluid L_α phase throughout the experiments. To investigate the influence of molecular chemistry (length and charge of oligosaccharide head groups) on the vertical and lateral structural ordering and mechanical properties of Lipid A and LPS membranes, neutron-scattering experiments were carried out under the following four conditions: (i) at low (~20%) relative humidity (corresponding to an osmotic pressure of $\sim 2.5\times 10^8$ Pa), (ii) at high (~95%) relative humidity ($\sim 8\times 10^6$ Pa), (iii) in Ca^{2+}-free buffer, and (iv) in Ca^{2+}-loaded buffer. Figure 4 (left) shows the reciprocal space map of LPS Ra multilayers at 60 °C and ~95% relative humidity. The integrated intensity of the second Bragg sheet as a function of $q_\parallel$ is also shown in the figure (right). Here, the sharpness of the central specular maximum (angular width of about 0.15°) indicates a remarkable alignment of the multilayers with the planar substrate.

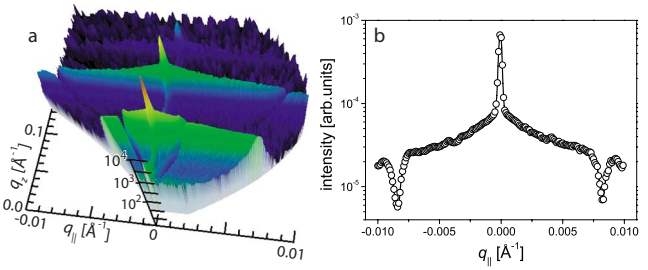

FIG. 4. (Color online) (a) Reciprocal space map, calculated according to Eq. (1) from data shown in Fig. 2. Here, the central line along $q_\parallel=0$ corresponds to the specular condition ($\Gamma=2\Omega$), while the regions of high intensity around periodic values of q_z result from the lamellar periodicity of the membranes and are known as Bragg sheets. (b) Integrated intensity of the second Bragg sheet as a function of $q_\parallel$. The sharp central maximum (angular width ~0.15°) evidences the high alignment of the membranes to the planar substrate.

A. Intermembrane interactions

The interactions between neighboring membranes are results of a complex interplay of various generic interactions [40], such as Coulomb, van der Waals, hydration, and steric interactions. Since the intermembrane interactions of Lipid A and LPS membranes are mediated via carbohydrate layers, hydrogen bonds between neighboring saccharides can be assumed to have an additional contribution [30,41]. Helfrich repulsion, caused by thermodynamic fluctuations, plays a crucial role in the interaction of weakly coupled membranes in smectic A (or L_α) phase. Therefore, experiments at various osmotic pressures enable us to study the influence of the intermembrane disjoining pressure [42,43] on the intermembrane interactions [44,45], while experiments in bulk buffers (corresponding to zero disjoining pressure) are a very powerful tool to study the effect of ions.

The lamellar periodicities d of Lipid A and LPS membrane multilayers, calculated from the positions of the Bragg peaks in the scattering signals, are summarized in Table II.

TABLE II. Lamellar spacings d of Lipid A and LPS multilayers subject to different osmotic pressures and buffer conditions at $T=60$ °C.

	~20% relative humidity	~95% relative humidity	Ca^{2+}-free buffer	Ca^{2+}-loaded buffer	50 mM $CaCl_2$
Lipid A	46.4 Å	47.5 Å	53.5 Å	47.6 Å	46.9 Å
LPS Re	49.4 Å	53.9 Å	unstable	50.5 Å	50.2 Å
LPS Ra	78.9 Å	83.2 Å	unstable	90.5 Å	90.4 Å

As a clear tendency, an increase in the lamellar periodicity according to the elongation of the saccharide head groups is observed under all the experimental conditions, which shows a reasonable agreement with previous reports [12,46]. Moreover, changes in the periodicity d between low (~20%) and high (~95%) humidities become more pronounced for the molecules with longer saccharide head groups ($\Delta d \sim 1$ Å for Lipid A, $\Delta d \sim 4.5$ Å for LPS Re and LPS Ra), reflecting their higher compressibility, since the larger and more complex head groups possess larger conformational degrees of freedom.

It is notable that only Lipid A forms stable multilayers in Ca^{2+}-free buffer with a finite spacing of $d=53.5$ Å. This implies that the attractive interactions (van der Waals, carbohydrate-mediated hydrogen bonds) between Lipid A membranes can overcome the electrostatic repulsion, since Lipid A has the lowest density of negatively charged groups among the studied systems. On the other hand, LPS Re and LPS Ra membranes are not able to form stable lamellae in Ca^{2+}-free buffer due to stronger electrostatic repulsion and due to the steric forces caused by the bulkier saccharide head groups. This finding is consistent with a previous diffraction study on LPSs [12], where no periodic ordering was found for LPS Re and LPS Ra membranes in Ca^{2+}-free buffer.

In contrast to the significant weakening of intermembrane confinement in Ca^{2+}-free buffer, Lipid A and both types of LPSs form stable, well-ordered multilayers in Ca^{2+}-loaded buffer, suggesting the tightening of intermembrane contacts in the presence of Ca^{2+}. In fact, the lamellar spacings of Lipid A ($d=47.6$ Å) and LPS Re ($d=50.5$ Å) are almost identical or even smaller than those at ~95% relative humidity, which corresponds to an osmotic pressure of almost 10^7 Pa. This tendency becomes even more prominent at high Ca^{2+} concentration (50 mM), where the spacings of Lipid A ($d=46.9$ Å) and LPS Re ($d=50.2$ Å) get close to those at 20% relative humidity, corresponding to an osmotic pressure of over 10^8 Pa. On the other hand, LPS Ra multilayers show a spacing of $d=90$ Å in Ca^{2+}-loaded buffer (5 mM $CaCl_2$), which is significantly ($\Delta d \sim 7$ Å) larger than that at ~95% relative humidity. This indicates that the longer and partially uncharged oligosaccharide moieties of LPS Ra resist to a certain extent the tightening of the intermembrane contact by Ca^{2+} ions due to their steric contribution.

B. Mechanical properties

While the position of the Bragg peaks yields the equilibrium periodicity of the mutant LPS membranes at given conditions, the mechanical properties of the interacting membranes can be calculated from the off-specular scattering signals. Here, the vertical (intermembrane) compression modulus B is a measure of how sharply the intermembrane potential confines the membranes between their neighbors. On the other hand, the bending rigidity κ reflects the lateral (intramembrane) interactions of the LPS molecules. Thus, B and κ can be used as quantitative indicators for the inter- and intramembrane interactions of Lipid A and LPSs.

In the following, we focus on the off-specular scattering results from the two most representative conditions: (1) at ~95% relative humidity, where very strong scattering signals can be recorded, and (2) in Ca^{2+}-loaded buffer, which provides the most biologically relevant environment for all the studied systems to form stable multilayers. In order to guarantee the validity of the first Born approximation, the second Bragg sheets are used for the comparison between experiments and simulations. Figure 5 shows a measured second Bragg sheet and the corresponding simulated intensity map, which was calculated using the best matching parameters. Since refraction and absorption effects, which are not considered in the first Born approximation, become important in the vicinity of the sample horizons (Yoneda wings [47], see Fig. 5 top image), this angular region was excluded from the comparison of experimental data and simulations. As presented in Fig. 6, Lipid A and LPS Ra show pronounced second Bragg sheets at high (~95%) relative humidity. This can be attributed to the increase in the scattering length density contrast according to the uptake of D_2O by the head groups. The intensities, integrated along Γ and plotted as a function of $q_{\|}$ (left panels), represent the displacement self-correlation function of an average membrane in the solid-supported multilayers, while the widths of the Bragg sheets along Γ, plotted as a function of $q_{\|}$ (right panels), represent the de Gennes parameter λ independent of the other parameters [48].[1] The parameters, including the mechanical parameters κ and B, used for the best fitting model (solid lines in Fig. 6) are summarized in Table III. The intensity of the second Bragg sheet of LPS Re (data not shown) is strongly suppressed due to the form factor corresponding to the scattering length density profile across the membranes, which prevents a quantitative analysis of the off-specular signals. The same problem occurs with Lipid A in Ca^{2+}-free buffer, where the periodicity is similar to that of LPS Re in ~95% relative humidity.

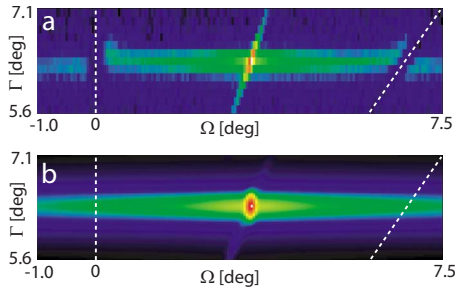

FIG. 5. (Color online) (a) Measured and (b) simulated second Bragg sheet in angular coordinates. The parameters η, λ, and R were adjusted to achieve the best agreement between simulations and experimental data. Data points near the sample horizons (indicated by dashed lines) were not used for the comparison.

The optimal R values used for the simulations (at the order of 1 μm) agree well with those reported for multilayers of synthetic glycolipids [30]. First, it is notable that the obtained bending rigidity of Lipid A ($\kappa=0.6k_BT$) is more than 2

[1]Due to the close relation between Γ and q_z, this is valid not only for the q_z-integrated intensity and the q_z width of the Bragg sheets, but also for the Γ-integrated intensity and the Γ width, in good approximation.

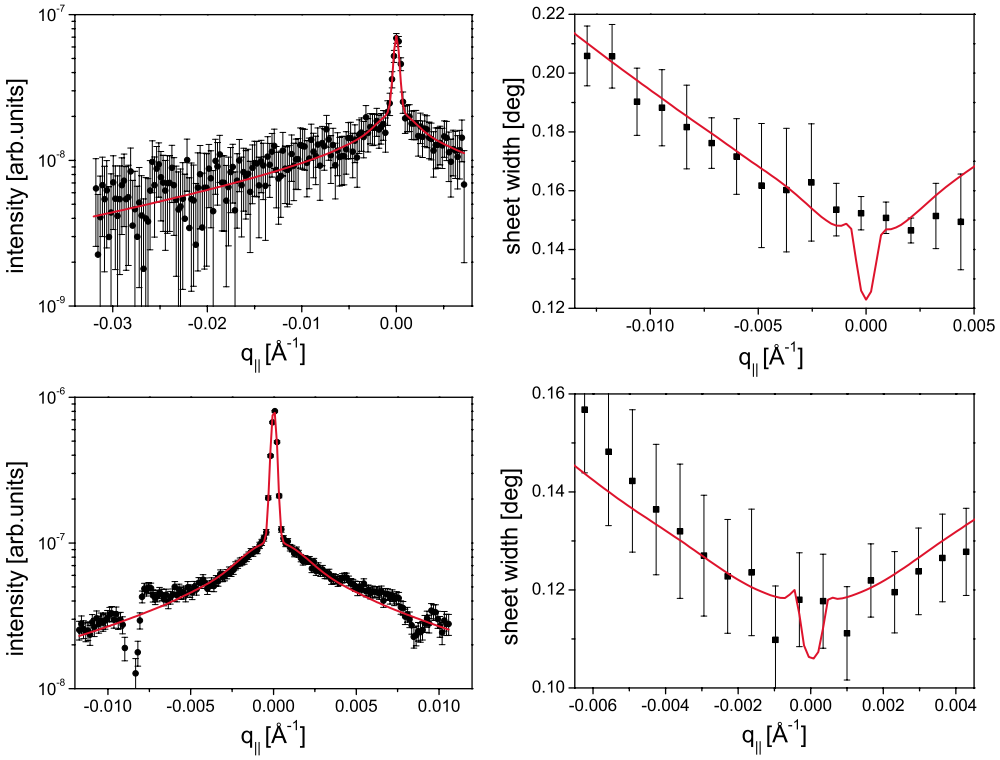

FIG. 6. (Color online) Measured scattering intensities (symbols) from the second Bragg sheets of Lipid A (top) and LPS Ra (bottom) membrane multilayers at 60 °C and ~95% relative humidity. Left panels: Bragg sheet intensity integrated along Γ and plotted as a function of $q_{||}$. Right panels: width (HWHM) of the Bragg sheets along Γ as a function of $q_{||}$. The parameters corresponding to the optimized models (solid lines) are summarized in Table III.

times smaller than that of LPS Ra ($\kappa=1.4k_BT$), indicating that the bulkier head groups of LPS Ra significantly rigidify the membranes. On the other hand, both values are by 1 order of magnitude smaller than the previously reported bending rigidities of synthetic phospholipid membranes [49–52]. This finding can be attributed to the molecular structure of Lipid A and LPSs. Bacterial lipids and LPSs have shorter hydrocarbon chains (with C10 and C12) than commonly studied phosphatidylcholine lipids (with C14 and C16), which can be assumed to result in a significant reduction of the bending rigidity [53]. Furthermore, if one considers the ratio between the cross-sectional areas occupied by hydrocarbon chains and saccharide head groups (known as packing parameter) [54], LPS membranes experience less sterical strain accommodating their head groups than phosphatidylcholine lipid membranes [55]. This would also result in a weaker contribution of the head groups to the bending rigidity of the whole membrane.

The obtained vertical compression moduli of Lipid A ($B=9$ MPa) and LPS Ra ($B=2.1$ MPa) seem to reflect the influence of the oligosaccharide head group structure on the intermembrane potential. The observed tendency clearly indicates that the intermembrane confinement of LPS Ra membranes is much softer than that of Lipid A membranes. This finding seems also plausible from the molecular structures, since the longer saccharide head groups of LPS Ra with their greater water uptake capability should possess a much higher compressional flexibility than the compact head groups of Lipid A.

Figure 7 shows experimental data for Lipid A (top) and LPS Ra (bottom) under Ca^{2+}-loaded buffer. The parameters corresponding to the optimized models (solid lines) are summarized in Table IV. As presented in the table, the bending rigidity of Lipid A ($0.8k_BT$) is about 2 times lower than that of LPS Ra ($1.7k_BT$), which are very similar to the corresponding values at ~95% relative humidity, κ (Lipid A) $=0.6k_BT$ and κ (LPS Ra)$=1.4k_BT$, respectively. This suggests that the lateral interactions of the saccharide head groups in Ca^{2+}-loaded buffer are similar to those at ~95% relative humidity (in the absence of liquid water). Similarly,

TABLE III. Parameters corresponding to the best matching simulations for Lipid A and LPS Ra membranes at $T=60$ °C and ~95% relative humidity.

	d	η	λ	R	κ	B
Lipid A	47.5 Å	0.135	2.5 Å	0.8 μm	$0.6k_BT$	9 MPa
LPS Ra	83.2 Å	0.08	6 Å	0.8 μm	$1.4k_BT$	2.1MPa

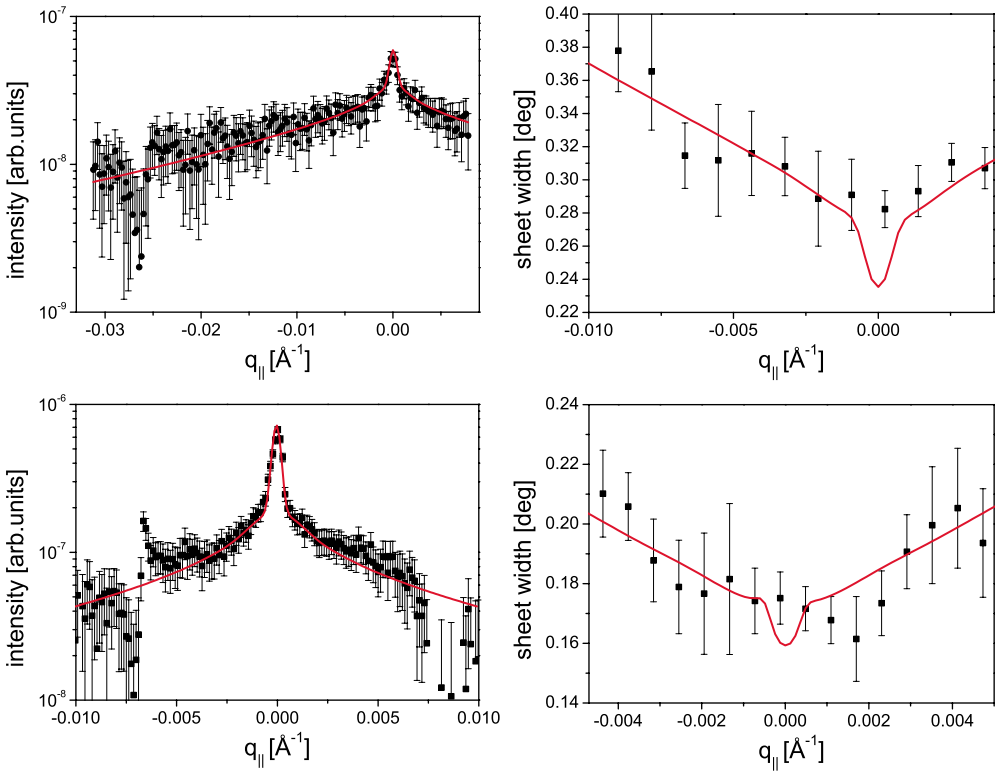

FIG. 7. (Color online) Measured scattering intensities (symbols) from the second Bragg sheets of Lipid A (top) and LPS Ra (bottom) membrane multilayers at 60 °C in Ca^{2+}-loaded buffer. Left panels: Bragg sheet intensity integrated along Γ and plotted as a function of $q_{||}$. Right panels: width (HWHM) of the Bragg sheets along Γ as a function of $q_{||}$. The parameters corresponding to the optimized models (solid lines) are summarized in Table IV.

the bending rigidity of neutral phospholipid membranes has been found to be largely independent of the water layer thickness by Pan *et al.* [56]. Unfortunately, it was not possible to extract the bending rigidity of LPS membranes in Ca^{2+}-free buffer due to the instability of the multilayers.

On the other hand, the compression moduli in Ca^{2+}-loaded buffer show clear differences from those at ~95% relative humidity. As presented in Table IV, the values in bulk buffer (B=5 MPa for Lipid A and B=1.1 MPa for LPS Ra) are approximately by a factor of 2 smaller than those at ~95% relative humidity. A clear decrease in the compression modulus can reasonably be attributed to a softening of the intermembrane potential by the presence of bulk water between the carbohydrate head groups. The dependence of the compression modulus B on the water layer thickness was systematically investigated by Pan *et al.* [56] for neutral phospholipid membranes and by Brotons *et al.* [22] for membranes composed of charged lipids. In fact, the compression modulus of LPS Ra membranes is comparable to that of membranes formed by synthetic glycolipids with neutral gentiobiose head groups in pure water (B =0.9 MPa) [30], which also swell by about 7 Å upon addition of bulk water. However, the decrease in the compression modulus of the synthetic glycolipids by pure water is much more significant (by a factor of 20). This indicates that the presence of Ca^{2+} between the charged carbohydrates of Lipid A and LPS molecules strengthens the intermembrane confinement, which is consistent with the fact that these systems are stabilized in the presence of Ca^{2+}.

IV. CONCLUSION

Complex glycolipids originated from bacteria were deposited on planar substrates to form oriented multilayers. These systems, hydrated in water vapor or in bulk buffers, serve as defined models to quantify intermembrane interactions and membrane bending rigidities using specular and off-specular neutron scattering. The observed equilibrium periodicities of the membranes show a systematic increase according to the elongation of the saccharide head groups. All studied mol-

TABLE IV. Parameters corresponding to the best-matching simulations for Lipid A and LPS Ra membranes at T=60 °C in Ca^{2+}-loaded buffer.

	d	η	λ	R	κ	B
Lipid A	47.6 Å	0.17	4 Å	1.0 μm	$0.8k_BT$	5 MPa
LPS Ra	90.5 Å	0.09	9 Å	1.2 μm	$1.7k_BT$	1.1MPa

ecules form stable, well-ordered multilayers in Ca^{2+}-loaded buffer, which is in contrast to a significant weakening of intermembrane confinement found in Ca^{2+}-free buffers. Furthermore, theoretical modeling of membrane displacement correlation functions including an effective cutoff radius allows for the simulation of the measured two-dimensional scattering signals as functions of the vertical compression modulus and the bending rigidity of the interacting membranes. We found that the elongation of saccharide head groups causes a significant softening of the intermembrane confinement but at the same time an increase in membrane bending rigidity by a factor of 2. The obtained results demonstrate the great potential of specular and off-specular neutron scattering for quantitative studies on the influence of various tunable parameters (degree of mutation, osmotic stress, ions, and specific molecules) on the structure and mechanics of complex biomembranes.

ACKNOWLEDGMENTS

We thank ILL (Grenoble) for the neutron beam time and T. Schubert for his assistance during the experiments. This work has been supported by the Deutsche Forschungsgemeinschaft (Contract No. Ta259/6) and the Fonds der Chemischen Industrie (M.T.). R.G.O. and F.R. thank Alexander von Humboldt Foundation for support and E.S. thanks the State Baden-Württemberg for support.

[1] O. Lüderitz, M. Freudenberg, C. Galanos, V. Lehmann, E. T. Rietschel, and D. H. Shaw, in *Membrane Lipids of Prokaryotes*, Vol. 17 of Current Topics in Membranes and Transport, edited by S. Razin and S. Rottem (Academic, New York, 1982), p. 79.
[2] T. D. Brock, Can. J. Microbiol. **4**, 65 (1958).
[3] L. Truelstrup Hansen, J. W. Austin, and T. A. Gill, Int. J. Food Microbiol. **66**, 149 (2001).
[4] N. M. D. Islam, T. Itakura, and T. Motohiro, Bull. Jpn. Soc. Sci. Fish. **50**, 1705 (1984).
[5] R. E. W. Hancock and D. S. Chapple, Antimicrob. Agents Chemother. **43**, 1317 (1999).
[6] R. G. Oliveira, E. Schneck, B. E. Quinn, O. V. Konovalov, K. Brandenburg, U. Seydel, T. Gill, C. B. Hanna, D. A. Pink, and M. Tanaka, C. R. Chim. **12**, 209 (2009).
[7] M. Kastowsky, T. Gutberlet, and H. Bradaczek, Eur. J. Biochem. **217**, 771 (1993).
[8] H. Labischinski, G. Barnickel, H. Bradaczek, D. Naumann, E. T. Rietschel, and P. Giesbrecht, J. Bacteriol. **162**, 9 (1985).
[9] N. Kato, M. Ohta, N. Kido, H. Ito, S. Naito, T. Hasegawa, T. Watabe, and K. Sasaki, J. Bacteriol. **172**, 1516 (1990).
[10] K. Brandenburg and U. Seydel, Biochim. Biophys. Acta **775**, 225 (1984).
[11] U. Seydel, K. Brandenburg, M. H. J. Koch, and E. T. Rietschel, Eur. J. Biochem. **186**, 325 (1989).
[12] S. Snyder, D. Kim, and T. J. McIntosh, Biochemistry **38**, 10758 (1999).
[13] T. A. Harroun, M. Koslowsky, M.-P. Nieh, C.-F. de Lannoy, V. A. Raghunathan, and J. Katsaras, Langmuir **21**, 5356 (2005).
[14] G. Pabst, H. Amenitsch, D. P. Kharakoz, P. Laggner, and M. Rappolt, Phys. Rev. E **70**, 021908 (2004).
[15] G. Pabst, M. Rappolt, H. Amenitsch, and P. Laggner, Phys. Rev. E **62**, 4000 (2000).
[16] C. R. Safinya, D. Roux, G. S. Smith, S. K. Sinha, P. Dimon, N. A. Clark, and A. M. Bellocq, Phys. Rev. Lett. **57**, 2718 (1986).
[17] C. R. Safinya, E. B. Sirota, D. Roux, and G. S. Smith, Phys. Rev. Lett. **62**, 1134 (1989).
[18] N. Lei, C. R. Safinya, and R. F. Bruinsma, J. Phys. II **5**, 1155 (1995).
[19] Y. Lyatskaya, Y. Liu, S. Tristram-Nagle, J. Katsaras, and J. F. Nagle, Phys. Rev. E **63**, 011907 (2000).
[20] L. Yang, T. A. Harroun, W. T. Heller, T. M. Weiss, and H. W. Huang, Biophys. J. **75**, 641 (1998).
[21] E. A. L. Mol, J. D. Shindler, A. N. Shalaginov, and W. H. de Jeu, Phys. Rev. E **54**, 536 (1996).
[22] G. Brotons, L. Belloni, T. Zemb, and T. Salditt, Europhys. Lett. **75**, 992 (2006).
[23] B. Pozo-Navas, V. A. Raghunathan, J. Katsaras, M. Rappolt, K. Lohner, and G. Pabst, Phys. Rev. Lett. **91**, 028101 (2003).
[24] M. C. Rheinstädter, C. Ollinger, G. Fragneto, F. Demmel, and T. Salditt, Phys. Rev. Lett. **93**, 108107 (2004).
[25] T. Salditt, J. Phys.: Condens. Matter **17**, R287 (2005).
[26] I. Koltover, T. Salditt, J.-L. Rigaud, and C. R. Safinya, Phys. Rev. Lett. **81**, 2494 (1998).
[27] T. Salditt, Curr. Opin. Struct. Biol. **13**, 467 (2003).
[28] T. Salditt and G. Brotons, Anal. Bioanal. Chem. **379**, 960 (2004).
[29] J. Pan, T. T. Mills, S. Tristram-Nagle, and J. F. Nagle, Phys. Rev. Lett. **100**, 198103 (2008).
[30] E. Schneck, F. Rehfeldt, R. G. Oliveira, C. Gege, B. Demé, and M. Tanaka, Phys. Rev. E **78**, 061924 (2008).
[31] T. Abraham, S. R. Schooling, M. Nieh, N. Kucerka, T. J. Beveridge, and J. Katsaras, J. Phys. Chem. B **111**, 2477 (2007).
[32] N. Kucerka, E. Papp-Szabo, M. Nieh, T. A. Harroun, S. R. Schooling, J. Pencer, E. A. Nicholson, T. J. Beveridge, and J. Katsaras, J. Phys. Chem. B **112**, 8057 (2008).
[33] C. Galanos, O. Lüderitz, and O. Westphal, Eur. J. Biochem. **9**, 245 (1969).
[34] E. T. Rietschel, H. W. Wollenweber, H. Brade, U. Zähringer, B. Lindner, U. Seydel, H. Bradaczek, G. Barnickel, H. Labischinski, and P. Giesbrecht, in *Handbook of Endotoxin*, edited by E. T. Rietschel (Elsevier, Amsterdam, 1984), Vol. 1, pp. 187–220.
[35] C. R. Raetz, R. J. Ulevitch, S. D. Wright, C. H. Sibley, A. Ding, and C. F. Nathan, FASEB J. **5**, 2652 (1991).
[36] K. Brandenburg, J. Andrä, M. Müller, M. H. J. Koch, and P. Garidel, Carbohydr. Res. **338**, 2477 (2003).
[37] B. Jiao, M. Freudenberg, and C. Galanos, Eur. J. Biochem. **180**, 515 (1989).
[38] W. Kern and D. A. Puotinen, RCA Rev. **31**, 187 (1970).
[39] S. K. Sinha, J. Phys. III (France) **4**, 1543 (1994).
[40] J. N. Israelachvili, *Intermolecular and Surface Forces*, 2nd ed.

(Academic Press Inc., London, 1991).
[41] I. Eggens, B. Fenderson, T. Toyokuni, B. Dean, M. Stroud, and S. Hakomori, J. Biol. Chem. **264**, 9476 (1989).
[42] B. V. Derjaguin and N. V. Churaev, *Surface Forces* (Consultants Bureau, New York, 1987).
[43] M. Tanaka, F. Rehfeldt, M. F. Schneider, G. Mathe, A. Albersdorfer, K. R. Neumaier, O. Purrucker, and E. Sackmann, J. Phys.: Condens. Matter **17**, S649 (2005).
[44] R. P. Rand and V. A. Parsegian, Biochim. Biophys. Acta **988**, 351 (1989).
[45] V. A. Parsegian, N. Fuller, and R. P. Rand, Proc. Natl. Acad. Sci. U.S.A. **76**, 2750 (1979).
[46] U. Seydel, M. H. J. Koch, and K. Brandenburg, J. Struct. Biol. **110**, 232 (1993).
[47] C. Münster, T. Salditt, M. Vogel, R. Siebrecht, and J. Peisl, Europhys. Lett. **46**, 486 (1999).
[48] T. Salditt, M. Vogel, and W. Fenzl, Phys. Rev. Lett. **90**, 178101 (2003).
[49] J. Daillant, E. Bellet-Amalric, A. Braslau, T. Charitat, G. Fragneto, F. Graner, S. Mora, F. Rieutord, and B. Stidder, Proc. Natl. Acad. Sci. U.S.A. **102**, 11639 (2005).
[50] E. Sackmann, in *Structure and Dynamics of Membranes*, edited by R. Lipowski and E. Sackmann (Elsevier, Amsterdam, 1995).
[51] H. I. Petrache, N. Gouliaev, S. Tristram-Nagle, R. Zhang, R. M. Suter, and J. F. Nagle, Phys. Rev. E **57**, 7014 (1998).
[52] W. Rawicz, K. C. Olbrich, T. McIntosh, D. Needham, and E. Evans, Biophys. J. **79**, 328 (2000).
[53] E. A. Evans, Biophys. J. **14**, 923 (1974).
[54] J. N. Israelachvili, D. J. Mitchell, and B. W. Ninham, J. Chem. Soc., Faraday Trans. 2 **72**, 1525 (1976).
[55] U. Seydel, M. Oikawa, K. Fukase, S. Kusumoto, and K. Brandenburg, Eur. J. Biochem. **267**, 3032 (2000).
[56] J. Pan, S. Tristram-Nagle, N. Kucerka, and J. F. Nagle, Biophys. J. **94**, 117 (2008).